Geomorphology xxx (2011) xxx–xxx

Contents lists available at SciVerse ScienceDirect

Geomorphology

journal homepage: www.elsevier.com/locate/geomorph

A comparison of permafrost prediction models along a section of Trail Ridge Road, Rocky Mountain National Park, Colorado, USA

Jason R. Janke [a,*], Mark W. Williams [b], Andrew Evans Jr. [a]

[a] Metropolitan State College of Denver CB 22, Denver, CO 80217, USA
[b] Institute of Arctic and Alpine Research, University of Colorado, CB 450, Boulder, CO 80309, USA

ARTICLE INFO

Article history:
Received 25 April 2011
Received in revised form 24 August 2011
Accepted 31 August 2011
Available online xxxx

Keywords:
Mountain permafrost
Soils
Front Range
Modeling
GIS
Uncertainty

ABSTRACT

The distribution of mountain permafrost along Trail Ridge Road (TRR) in Rocky Mountain National Park, Colorado, was modeled using 'frost numbers' and a 'temperature of permafrost model' (TTOP) in order to assess the accuracy of prediction models. The TTOP model is based on regional observations of air temperature and heat transfer functions involving vegetation, soil, and snow; whereas the frost number model is based on site-specific ratios of ground temperature measurements of frozen and thawed degree-days. Thirty HOBO© temperature data loggers were installed near the surface as well as at depth (30 to 85 cm). From mid-July 2008 to 2010, the mean annual soil temperature (MAST) for all surface sites was −1.5 °C. Frost numbers averaged 0.56; TTOP averaged −1.8 °C. The MAST was colder on western-facing slopes at high elevations. Surface and deeper probes had similar MASTs; however, deeper probes had less daily and seasonal variation. Another model developed at the regional scale based on proxy indicators of permafrost (rock glaciers and land cover) classified 5.1 km^2 of permafrost within the study area, whereas co-kriging interpolations of frost numbers and TTOP data indicated 2.0 km^2 and 4.6 km^2 of permafrost, respectively. Only 0.8 km^2 were common among all three models. Three boreholes drilled within 2 m of TRR indicate that permafrost does not exist at these locations despite each borehole being classified as containing permafrost by at least one model. Addressing model uncertainty is important because nutrients stored within frozen or frost-affected soils can be released and impact alpine water bodies. The uncertainty also exposes two fundamental problems: empirical models designed for high latitudes are not necessarily applicable to mountain permafrost, and the presence of mountain permafrost in the alpine tundra of the Colorado Front Range has not been validated.

1. Introduction

Mountain permafrost is highly sensitive to changing air temperature; it affects the depth of thaw of the annual active layer as well as the timing and rate of refreezing (Leopold et al., 2010). Clow (2010) showed that mean annual air temperature (MAAT) at high elevations in the Colorado Front Range has increased by 1.0 °C per decade from 1983 to 2007 and that the timing of snowmelt is two to three weeks earlier in the year. According to Hoffman et al. (2007), this increase in air temperature is the primary cause of glacial retreat in the Colorado Rockies, although most glaciers are small, fed by blowing snow, and located in shaded, protected cirques. Late-season discharge at these high-elevation catchments has increased, suggesting that melting of ice previously stored within mountain permafrost from talus and rock glaciers is being released (Williams, 2009; Williams et al., 2009; Caine, 2011).

Thawing of permafrost in high elevation catchments may cause unanticipated changes in ecosystem processes. For example, Baron et al. (2009) explored the consequences of the warming trend on nitrate in streams in alpine and subalpine watersheds that have long been the recipient of elevated atmospheric nitrogen (N) deposition. They concluded that the observed recent N increases in streams draining the Loch Vale catchment are the result of warmer summer and fall mean temperatures, which melts ice in glaciers and rock glaciers. This, in turn, has exposed sediments from which N produced by nitrification can be flushed. Aeolian sediments being deposited on the rock glaciers could be another source of N. Similarly, Williams et al. (2006, 2007) showed that enhanced melt of ice in rock glaciers can cause an unexpected flushing of nitrate to high elevation streams.

Changes in the extent of permafrost can cause localized slumping, loss of soil cohesion from melting ice, or subsidence, which could pose a threat to infrastructure such as roads, buildings, ski lifts, or communication towers (Isaksen et al., 2007; Lantz and Kokelj, 2008). Thus, the spatial extent of mountain permafrost in the western USA must be

* Corresponding author. Tel.: +1 303 556 3072; fax: +1 303 556 4436.
E-mail addresses: jjanke1@mscd.edu (J.R. Janke), markw@snobear.colorado.edu (M.W. Williams), aevans24@mscd.edu (A. Evans).

0169-555X/$ – see front matter © 2011 Elsevier B.V. All rights reserved.
doi:10.1016/j.geomorph.2011.08.029

determined with greater certainty. Regional projections of permafrost extent in the Front Range of Colorado have been developed based on climate change scenarios (Janke, 2005b). A 2.0 to 2.5 °C temperature increase could dramatically reduce permafrost extent by about 95% in the Front Range (Janke, 2005b). The loss of permafrost may have a large effect on ecosystem health of protected areas such as those in Rocky Mountain National Park. Moreover, the National Park Service has expressed concerns that several sections of Trail Ridge Road (TRR), the highest continuous paved road in the United States, could buckle, subside, or crack from melting ice within permafrost.

A combination of geomorphological, hydrological, physical, and proxy indicators have been used to map permafrost extent (Damm and Langer, 2006; Etzelmüller et al., 2007). Multicriteria geographic information system (GIS) techniques and proxy indicator data related to frozen ground–such as rock glaciers, active patterned ground, thermokarst, pingos, solifluction lobes, tundra vegetation, or other land cover types–have been used to map extent (Grosse et al., 2005; Janke, 2005a; Nyenhuis et al., 2005; Etzelmüller et al., 2006). Direct measurements through boreholes, temperature sensors placed in the active layer, and basal temperature of winter snow (BTS) have also been used (Gruber and Hoelzle, 2001; Lewkowicz and Ednie, 2004; Pieracci et al., 2008; Ridefelt et al., 2008). Indirect methods have utilized thermal remote sensing, such as MODIS data, to calculate near surface temperatures (Hachem et al., 2009). Electrical conductivity, ground penetrating radar (GPR), or other geophysical techniques that reveal a distinct difference between frozen and unfrozen ground provide important information about depth to permafrost but are somewhat spatially limited (Munroe et al., 2007; Fukui et al., 2008; Leopold et al., 2008, 2010; Schrott and Sass, 2008; Degenhardt, 2009).

Because of the lack of direct measurements of permafrost, Nelson and Outcalt (1987) developed the frost number–a dimensionless ratio defined by manipulation of either freezing and thawing degree-day sums or frost and thaw penetration depths–to define an unambiguous latitudinal zonation of permafrost. The index was computed using several variables influencing the depth of frost and thaw penetration and can be related mathematically to the existence and continuity of permafrost in the Arctic. They show that a frost number >0.5 as the 'permafrost limit.'

Smith and Riseborough (2002) integrated air and surface temperatures with seasonal surface transfer functions based on vegetation and snow cover as well as soil thermal conductivity to develop the temperature of permafrost (TTOP) model. Using data from climate stations across Canada, discontinuous and continuous permafrost were mapped. The results corresponded with the −6° and −8 °C isotherms, respectively. They found that the ground thermal conductivity ratio between thawed and frozen states is the critical factor for determining the southern limit of discontinuous permafrost, whereas snow cover is critical for determining the northern limit of discontinuous permafrost in Arctic regions. These techniques, however, may not be applicable to mountain permafrost.

A dense network of direct measurements of temperature could provide a valuable method to map and monitor permafrost and environmental conditions along TRR. Local models of distribution could also be compared with regional models to address issues of scale, appropriateness of proxy data sources, and uncertainty. The objectives of this study were to

(i) develop a detailed, local account of the potential permafrost distribution along TRR using the frost number and temperature of permafrost methods; and
(ii) compare these permafrost model results with an existing regional model based on rock glacier distribution and land cover characteristics and borehole temperature measurements to improve estimates of the spatial distribution of potential permafrost in the Colorado Front Range.

2. Study area

Trail Ridge Road (TRR) extends along a 9.7-km, gently sloping (2 to 25°) periglacial interfluve surface (Fig. 1). Within the study area, elevations range from 3682 m on the eastern side of TRR to 3517 m on the western side. The mean elevation along the road is 3620 m; the highest point is situated at 3713 m (Fig. 1). The road is exposed to a variety of aspects; southern- and western-facing slopes are common as the road parallels the Big Thompson River (south of Fig. 1), but as the road veers north, northwestern-facing slopes are more abundant. About 25% of the road has northwestern aspects; 22% faces southwest; and 18% faces south. Slope averages about 12° across the road, whereas mean curvature of the interfluve is slightly convex at 0.16. Most soils have a slightly acidic pH (5 on average), which may be the result of acid precipitation, particularly from accumulations of snow. Bulk densities average about 1.12 g/cm^3; and porosity averages about 48%, a typical value for a silt to clay loam soil. Alpine tundra borders most sections of the road, although certain sections cut through bedrock and talus accumulations. Earth hummocks, perennial snow patches, patterned ground, rock wedges, stone stripes, and solifluction lobes are present.

A comparable alpine tundra environment exists about 40 km to the south at the D-1 Long-Term Ecological Research (LTER) climate station (3739 m) on Niwot Ridge (Table 1). From 1952 to 2004, MAAT has averaged about −3.5 °C, and precipitation totals average 94 cm/y. The last ten years of measurements of air and soil temperature for D-1 are summarized in Table 1. According to the closest SNOTEL (snowpack telemetry) site, Willow Park at 3294 m (below tree line), snow accumulates by mid-October and melts by mid-June. The site receives 100 cm of precipitation annually. In Rocky Mountain National Park, the Loch Vale watershed extends from 3097 m (forested) to 4009 m (alpine tundra) at Taylor Peak; MAATs range from 1.7 °C at the basin outlet to an estimated −5.0 °C at Taylor Peak (Clow et al., 2003). Mean annual precipitation in the Loch Vale watershed is 110 cm, of which 65% to 85% falls as snow (Baron and Denning, 1993). Above tree line in the tundra ecosystem, the spatial variability of snow is high as strong winds redistribute snow in hollows and eastern-facing cirques.

3. Methods

3.1. Field installation of sensors

Thirty HOBO© temperature data loggers with internal and external sensors were installed in areas of potential permafrost along TRR during July 2008 (Fig. 1). Holes were drilled using a standard soil auger, sensors were inserted, and the holes were backfilled. Surface sensors were installed at a depth of 10 cm, whereas external sensor depths ranged from 30 to 85 cm; depth was controlled by the rock content of the site. For each sensor location, elevation, slope, and aspect were measured (Table 2). Loggers were launched and set to record temperature at 2-h intervals.

Three boreholes were drilled to 6 m depth in July 2010 (Fig. 1). Temperature data loggers were placed at 1 m intervals. Large trucks required for drilling limited site selection—driving across the tundra was not permitted and space was limited in parking lots or pullovers. Each borehole was drilled within 2 m of TRR in tundra vegetation and was backfilled with a thermally inert grout. Borehole 1 was drilled near site 4; borehole 2 was drilled near the tundra communities trail; and borehole 3 was drilled in a median between TRR and the Gore Range parking lot (Fig. 1).

3.2. Calculations

During July 2010, the thirty temperature loggers were relocated and data were downloaded. Only four of sixty temperature sensors

Please cite this article as: Janke, J.R., et al., A comparison of permafrost prediction models along a section of Trail Ridge Road, Rocky Mountain National Park, Colorado, USA, Geomorphology (2011), doi:10.1016/j.geomorph.2011.08.029

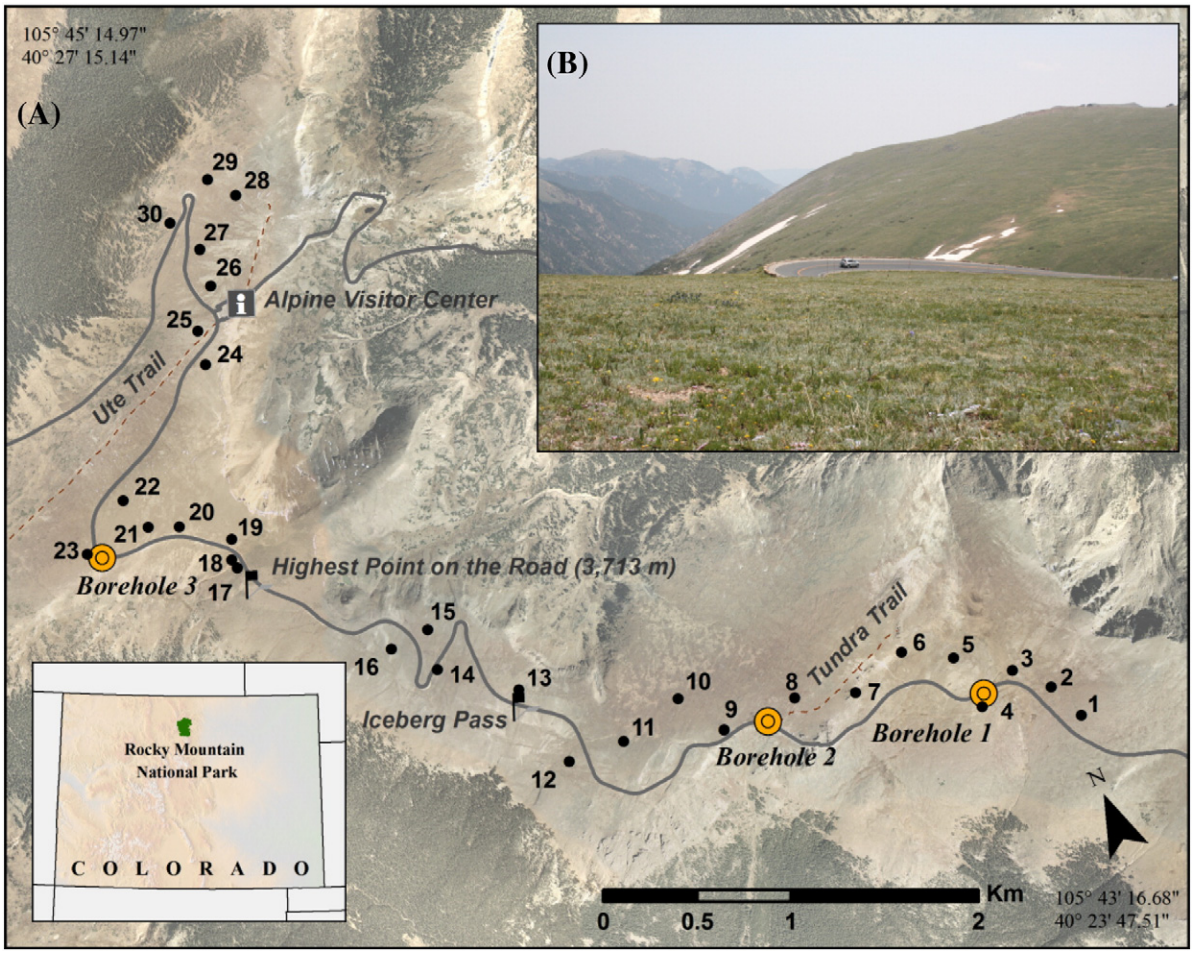

Fig. 1. (A) Location of the study area along Trail Ridge Road (TRR) in Rocky Mountain National Park, Colorado, USA; and (B) a terrestrial photograph illustrating the gently sloping tundra surfaces. The photo was taken from point 11 facing west.

contained erroneous readings. Using two years of data, frost numbers (F) were calculated with the following formula:

$$F = \frac{DDF^{1/2}}{DDF^{1/2} + DDT^{1/2}} \quad (1)$$

where, DDF is the degree-day sum as a positive number for frozen states; and DDT is the degree-day sum for thawed states. Values of F are, thus, restricted to the closed interval [0,1]. Greater numbers indicate better probability of permafrost occurrence.

Two years of surface and deeper (30 to 85 cm) temperature measurements and measurements of air temperature from nearby Niwot Ridge (adjusted for elevation) were input into the following equation to estimate the temperature at the top of the permafrost layer. The TTOP measurements <0 °C indicate permafrost presence:

$$TTOP = \frac{(rk \times nt \times It) \times (nf \times If)}{P} \quad (2)$$

Table 1
Climatic data for air and soil temperature at the D-1 site on Niwot Ridge, CO.[a]

		2000–2001	2001–2002	2002–2003	2003–2004	2004–2005	2005–2006	2006–2007	2007–2008	2008–2009	2009–2010
Air temperature (°C)	Average	−2.4	−1.9	−2.5	−3.2	−2.4	−2.1	−2.2	−3.0	−2.2	−3.6
	Standard deviation	9.1	9.4	8.7	8.6	7.9	9.2	8.7	8.7	8.5	8.9
	Minimum	−20.6	−27.1	−22.7	−24.5	−25.7	−26.6	−24.8	−24.8	−23.8	−26.5
	Maximum	13.1	14.6	13.9	14.0	12.9	15.1	14.5	14.5	14.5	13.0
	Count (n)	359	365	362	319	360	362	364	364	365	343
Soil temperature (°C)	Average	−0.9	−0.5	−1.6	−0.8	−0.8	−0.6	−0.9	−1.3	−0.8	−1.7
	Standard deviation	6.9	7.2	8.4	6.4	6.0	7.0	6.6	6.6	6.1	6.7
	Minimum	−11.9	−13.9	−18.9	−11.8	−12.7	−12.5	−14.4	−14.4	−11.9	−13.7
	Maximum	11.8	14.4	14.6	13.7	11.3	12.3	11.4	11.4	11.2	9.9
	Count (n)	358	365	364	325	362	362	364	364	365	358

[a] Data courtesy of the Niwot Ridge LTER data page, Mark Losleben, INSTAAR, CB 450, University of Colorado, Boulder.

Please cite this article as: Janke, J.R., et al., A comparison of permafrost prediction models along a section of Trail Ridge Road, Rocky Mountain National Park, Colorado, USA, Geomorphology (2011), doi:10.1016/j.geomorph.2011.08.029

Table 2
Characteristics of sample points.

Point	Point description	Aspect (direction)	Elevation (m)	Slope (°)
1	Rock wedge	SW	3688	19
2	Side of solifluction lobe	WSW	3690	15
3	Earth hummock	SSW	3684	4
4	Tundra	SE	3677	14
5	Tundra	NE	3707	13
6	Downslope from snowpack	SSE	3724	12
7	Tundra below rock outcrop	SE	3736	17
8	Center of rock wedge	NW	3711	7
9	Tundra	W	3685	7
10	Solifluction step	N	3651	12
11	Center of rock wedge	NNW	3647	8
12	Tundra	W	3607	19
13	Wet slump	NE	3614	14
14	Frost heaving	SE	3665	8
15	Tundra with stone stripes	E	3678	13
16	Exposed tundra surface	SSE	3692	2
17	In between stone stripes	W	3702	25
18	Coarse rock	W	3700	24
19	Tundra	SW	3733	19
20	Stone stripes	SW	3720	10
21	Tundra	W	3699	6
22	Active heave	N	3675	15
23	Tundra	NW	3658	10
24	Rocky mixture in tundra	NNW	3625	23
25	Rocky mixture in tundra	NW	3580	17
26	Tundra	WNW	3604	13
27	Disturbed soil	NW	3590	18
28	Stone stripes	N	3603	18
29	Bog-sedge-alder	N	3565	10
30	Tundra	NW	3530	17

where, *rk* is a ratio of thermal conductivity during the thawed and frozen states; *nt* is the summer scaling factor between the air temperature and ground surface temperature to adjust for vegetation cover; *It* is the degree-days for thawed conditions; *nf* is a winter scaling factor between the air temperature and ground surface temperature to account for the effects of snow; *If* is the degree-days for frozen conditions, expressed as a positive number; and *P* is the number of days in the record (Smith and Riseborough, 2002).

3.3. Spatial interpolation

Frost numbers and TTOP for the thirty sites were used to model the probability of occurrence of permafrost using GIS techniques. Kriging methods were evaluated for their effectiveness at interpolating the frost number and TTOP values. Ordinary co-kriging with a spherical model was used to interpolate the frost numbers and estimates of TTOP across the study area because of low root mean square errors and standard errors. Elevation, slope, curvature, and aspect were used as secondary variates for the co-kriging models. Each model was then spatially adjusted using a landcover weighting procedure based on perennial snow cover calculated from a Landsat 5 image from late May (5/25/2006). This image represented areas that experience developed snow cover over the winter months, thus restricting the formation of permafrost. The TTOP areas that intersected the snow layer were adjusted by +0.7 °C, whereas frost numbers were reduced by 0.06. These values were calculated by evaluating surface sensor measurements for snow-free and snow-covered areas for the winter months. Finally, grids were queried for frost numbers >0.50 and TTOP estimates <0 °C to estimate the extent of potential permafrost occurrence.

4. Results

4.1. Temperature measurements

Soil temperatures ranged from a maximum temperature of 26.5 °C to a minimum temperature of −21.8 °C from mid-July 2008 to mid-July 2010. The mean annual soil temperature (MAST) for all surface sites was −1.5 °C. Soil temperatures from July 2009 to July 2010 were about 0.5 °C cooler on average compared to those from July 2008 to July 2009. Minimum and maximum temperatures were greater at the surface sensor compared to deeper probes. Maximum temperatures occurred in mid-July to early August, whereas minimum temperatures were recorded at the end of December for most sites. Examples of temperature plots at site 1 and site 3 are provided in Fig. 2. Site 1 consists of blocky material within a rock wedge; site 3 was drilled in an earth hummock. Each has similar elevation and aspect but site 1 has a significantly steeper slope (Table 2).

4.2. Effects of snow

In the Front Range, the timing and redistribution of snow affects ground temperatures. Winter soil temperature means (Dec.–Feb.) were −7.0 °C. One date (1/17/09) averaged about −9.5 °C for sites that were snow free and about −7.0 °C for sensors that were fully covered with snow (depth information not available). Snow cover as thin as 25 to 50 cm can warm the ground (Williams and Smith, 1989; Monson et al., 2006). After examining satellite imagery and visiting sites in the early spring, twenty of thirty sites are typically windswept and are covered by no- or thin-winter snow <10 cm in depth. During the winters of each year, snow-free sites were 1.8 °C colder on average and had greater standard deviations. Snow-free areas averaged −9.4 °C, and snow-covered sites averaged −7.5 °C, well below the −3.0 °C BTS threshold that is indicative of permafrost presence. March through mid-April averages were −5.4 °C for snow-covered sites. A transition occurs in March: areas with no snow warmed to −6.6 °C, whereas fully covered areas of snow warmed less to −5.4 °C. Additional spring snowfall may be an important factor for permafrost occurrence because of its ability to extend the cold season, protecting underlying ground from summer insolation; however, spring snowmelt continues to occur earlier in the season (Clow, 2010).

4.3. Frost numbers and TTOP estimates

Frost numbers ranged from 0.54 to 0.60, with a mean value of 0.56 (calculated from Eq. 1). Additionally, the soil is frozen for the majority of days (>183 days) during the year. These frost numbers indicate a possibility for permafrost at all sites (Fig. 3). From Eq. (2), the TTOP model suggests that permafrost is present at all sites except site 13 (TTOP = 1.1 °C) near Iceberg Pass (Fig. 4). Permafrost temperatures ranged from −0.3° to −3.4 °C, with a mean value of −1.8 °C for all sites.

4.4. Spatial interpolation

A comparison of the co-kriging models (frost number and TTOP) and the original permafrost model (only the probable class included because of its greater certainty) from Janke (2005a) are shown in Fig. 5 and Animation 1. Table 3 provides accuracy information about the co-kriging interpolation method. In terms of areal extent of classified permafrost, the original model is the most liberal and the frost number model is most restrictive. The original model suggested that 78% of TRR is underlain by permafrost; the TTOP model classified 71% of the area under TRR as permafrost; and the frost number model categorized 44% of TRR as underlain with permafrost (Table 4). According to the original model, probable permafrost extends to lower elevations along eastern aspects, whereas the frost numbers and TTOP data suggest that permafrost more likely exists at lower elevations on western-facing slopes (Fig. 5).

Please cite this article as: Janke, J.R., et al., A comparison of permafrost prediction models along a section of Trail Ridge Road, Rocky Mountain National Park, Colorado, USA, Geomorphology (2011), doi:10.1016/j.geomorph.2011.08.029

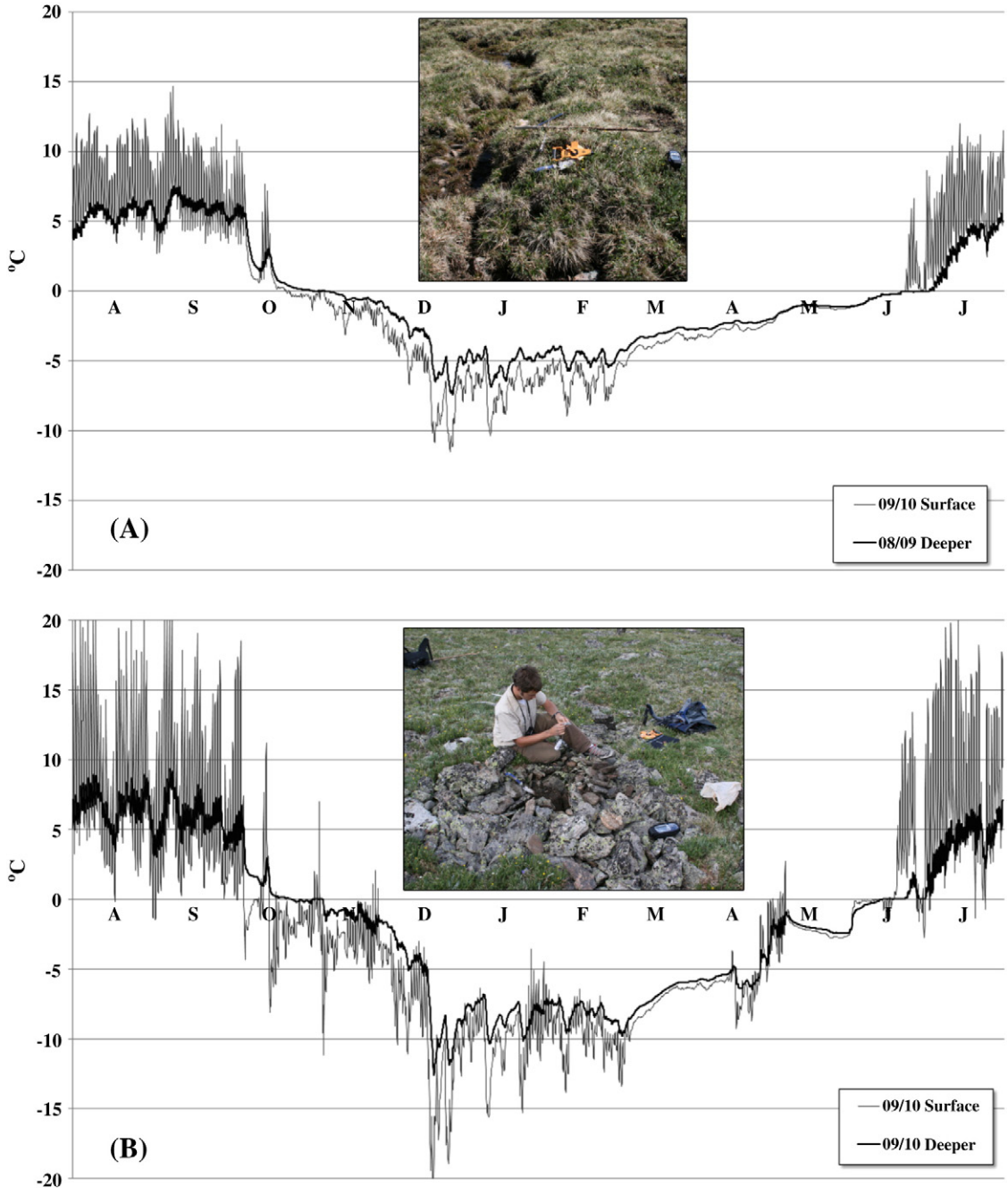

Fig. 2. Temperature plots from August 2009 through July 2010 for Site 3 and Site 4. Site 3 (A) consists of organic soil located in a series of earth hummocks; site 4 (B) is located in the center of a rock wedge. The two sites are <0.5 km from each other.

5. Discussion

5.1. BTS validity in the Front Range

Hoelzle et al. (1993) and Lewkowicz and Ednie (2004) suggested that a BTS below −3.0 °C indicates the presence of permafrost at depth. The BTS rule-of-thumb was designed for the European Alps, which vary considerably in terms of topography and climate compared to the Rocky Mountains where snowfall totals are generally less and variability is high. According to winter month means, twenty-nine of thirty sites should have permafrost; however, a deep snowpack often does not exist. Underrepresented aspects or elevations, late snow cover, mid-winter melt, different subsurface conditions (voids in rocks, tundra, bare soil, etc.), or different scales can cause variance to occur in BTS measurements; as a result, uncertainty is likely to exist (Brenning et al., 2005). Lewkowicz and Bonnaventure (2008) compared two areas more than 200 km apart in northwest Canada and found that BTS predictions were within 2% of each other; however, for other dissimilar areas, the BTS method did not remain valid (Bonnaventure and Lewkowicz, 2008). The high variability of alpine permafrost makes such simple generalizations difficult to extrapolate over great distances. On rock glaciers, the range of autocorrelation of BTS measurements could be as short as 20 m (Brenning et al., 2005). For the area around TRR, a semivariogram suggested spatial autocorrelation of MAST had a range of 1500 to 2300 m. Proper site selection and extensive ground truthing are necessary.

Please cite this article as: Janke, J.R., et al., A comparison of permafrost prediction models along a section of Trail Ridge Road, Rocky Mountain National Park, Colorado, USA, Geomorphology (2011), doi:10.1016/j.geomorph.2011.08.029

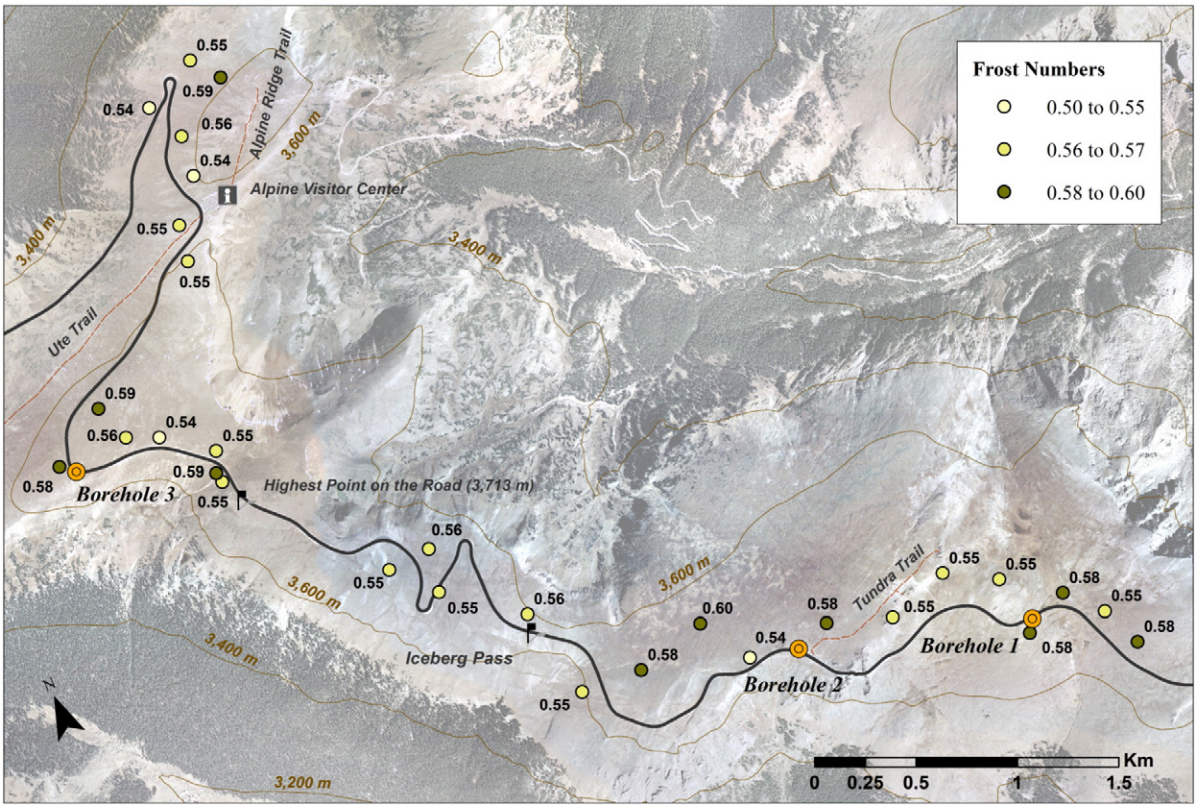

Fig. 3. Frost numbers for sites along Trail Ridge Road (TRR) calculated from Eq. (1).

5.2. Environmental variables affecting permafrost

Steeper slopes and convex curvatures had lower MASTs. This is related to snow distribution, as less snow is likely to accumulate on steep slopes and ridges or because the slopes consist of coarse rocks in which cold air may settle through Balch ventilation (Haeberli, 1985). Western and northern slopes had lower MASTs compared to southern and eastern aspects. Interestingly, western-facing slopes

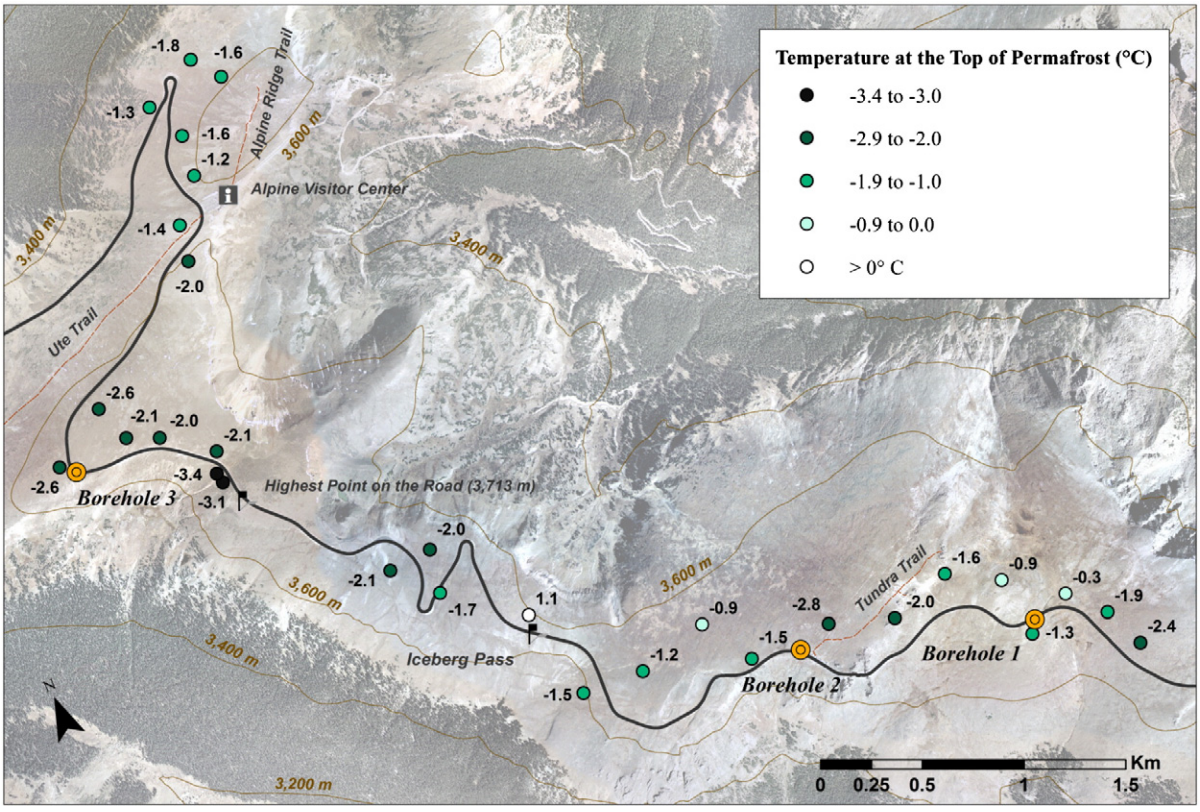

Fig. 4. Temperature at the top of permafrost according to calculations from Eq. (2).

Please cite this article as: Janke, J.R., et al., A comparison of permafrost prediction models along a section of Trail Ridge Road, Rocky Mountain National Park, Colorado, USA, Geomorphology (2011), doi:10.1016/j.geomorph.2011.08.029

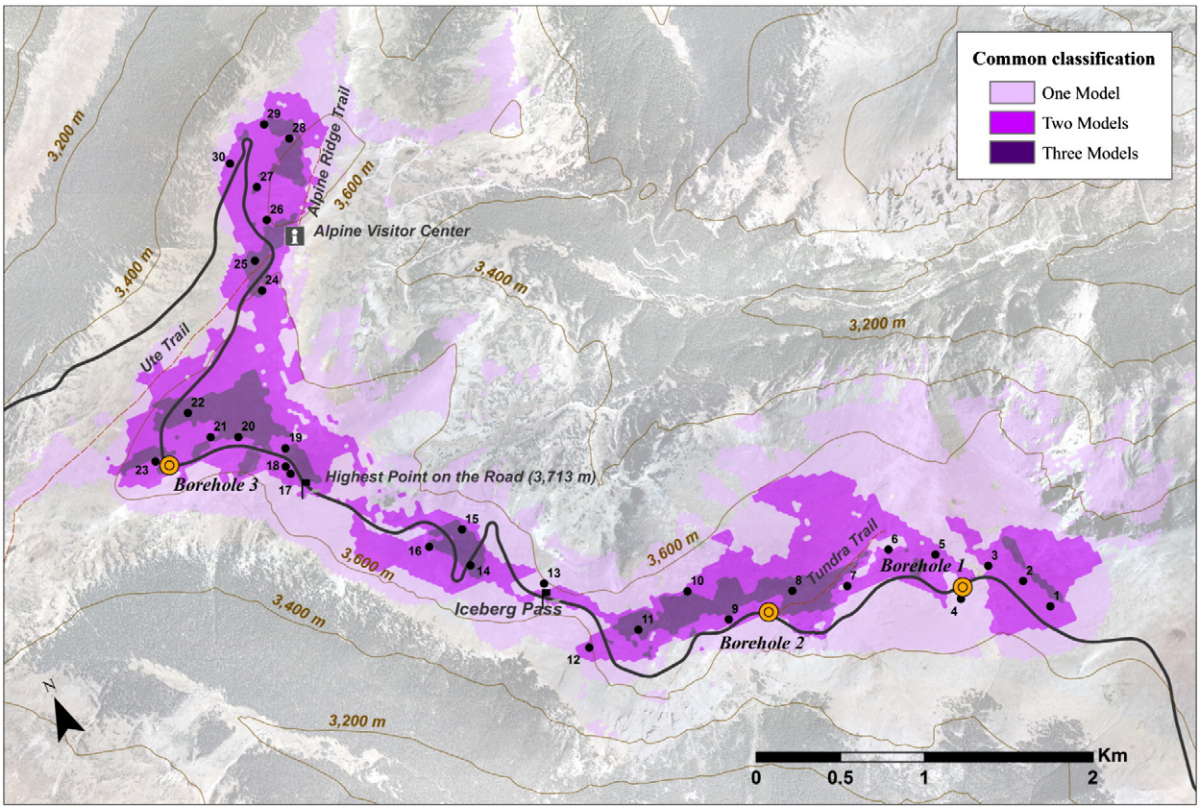

Fig. 5. A comparison of three permafrost prediction models. Darker values indicate greater certainty in terms of common area classified as permafrost for each model. The area common to each model was only 0.75 km^2.

had greater frost numbers; however, this may be the result of limited samples on northern-facing slopes. Wind direction in the Colorado Front Range during the winter is predominately from the west and northwest (Erickson et al., 2005). As a result, scouring of snow on western- and northwestern-facing slopes leads to minimal snow accumulation and, therefore, less insulation at these sites during the winter months. Soils are colder when compared to nearby sites with a developed snowpack; therefore, colder ground temperatures can extend to lower elevations on northwestern-facing slopes.

Soil properties were not correlated with MAST. Porosity could affect permafrost formation by two means. First, soils with low porosities (sands) should have greater thermal conductivities; greater porosities (clays) should have lower thermal conductivities (Abu-Hamdeh and Reeder, 2000; Smits et al., 2010). Greater thermal conductivity is advantageous for permafrost formation because it allows cold air to penetrate deeply into the soil. Second, greater porosities lead to greater potential for water storage. Soils with greater moisture content should have greater thermal conductivities (by as much as 10 times) compared to dry soils (Abu-Hamdeh and Reeder, 2000). Ice content increases the thermal conductivity more compared to water. The relatively low thermal conductivity and high porosity of the research area are both conducive to the formation of permafrost, but showed no statistically significant relationship to MAST.

5.3. Comparison of modeling methods

Table 5 provides area estimates of permafrost extent for each of the models. Of the area shown in Fig. 5, estimates of permafrost extent range from 1.99 to 5.08 km^2, with only 0.75 km^2 common to each model. The high uncertainty between the models is a product of the empirical model inputs. The models presented here are best described at the scales from which data inputs were obtained: macro (original model), meso (TTOP), and micro (FI). The original model was developed at the macroscale, based on indicator criteria (rock glaciers); the TTOP relies on local ground temperature measurements, landcover characteristics, heat transfer functions, and regional air temperature measurements (obtained from the D-1 station on Niwot Ridge); and the frost number model is based on local degree-day ratios at each point.

The original permafrost prediction model based on rock glacier occurrence was developed at the regional scale and, as a result, omits local variation and overestimates when compared with the local data, especially in non-rocky areas. At the regional level, the effects of topography, such as elevation and direct radiation, are important; whereas at local scales, soil properties, vegetation, and snow cover are more important (Brenning et al., 2005). Rock glaciers overestimate regional permafrost distribution because their average temperatures are colder than surrounding areas. Balch ventilation will cause cold air to settle in void spaces, creating a microclimate that does not represent the overall regional climate (Pieracci et al., 2008). Such differences in model inputs become apparent when attempting to extrapolate results to flat Tertiary periglacial surfaces with tundra grasses and thin soils—the environment in which frost numbers and TTOP model inputs were obtained.

The high disagreement among models suggests that spatial interpolation from site-specific point data may not be possible or

Table 3
Co-kriging model results.

	Lag distance (m)	Range	Nugget	Sill	Method	Model	Root mean square error	Standardized error
Frost number model	200	2348	1.45	2.74	Ordinary co-kriging	Spherical	1.08	0.9872
TTOP model	200	1578	1.23	1.95	Ordinary co-kriging	Spherical	1.12	−0.0002

Please cite this article as: Janke, J.R., et al., A comparison of permafrost prediction models along a section of Trail Ridge Road, Rocky Mountain National Park, Colorado, USA, Geomorphology (2011), doi:10.1016/j.geomorph.2011.08.029

Table 4
Model estimates of length of Trail Ridge Road underlain by permafrost.

	Length of Trail Ridge Road underlain by permafrost (km)		Percentage of road shown (%)	
Original model	3.2 (probable) 5.7 (possible)	8.9 (total)	28 (probable) 50 (possible)	78 (total)
Frost number model	5.0		44	
Temperature of permafrost model	8.1		71	

permafrost may not exist at most of these locations. Modeling results need additional verification in the field because of the high variability of Front Range permafrost. For example, several studies suggest that the D-1 site along Niwot Ridge contains permafrost (Table 1) (Ives and Fahey, 1971; Ives, 1974; Janke, 2005a). According to the original model, results suggest a 63% probability of permafrost occurrence at D-1 (Janke, 2005a). However, through an electric resistivity tomography survey, Leopold et al., (2010) found no evidence of ice from the surface to 10 m depth near D-1. Boreholes lined with temperature data loggers would provide additional direct measurement of permafrost presence along TRR.

Borehole temperature data are provided in Fig. 6. Soil temperatures remain above freezing from the surface to 6 m depth at each location. In addition, the range of temperature extends to above freezing at all depths and locations. This indicates permafrost does not exist at these locations; however, the asphalt road may affect permafrost formation. Comparing the borehole locations with model results creates more concern. The TTOP model predicted permafrost at all three boreholes; the frost number model predicted permafrost at boreholes 2 and 3; and the original model suggested permafrost at borehole 3. The lack of agreement raises the question of whether these models are useful to predict permafrost in the alpine tundra or, more importantly, whether mountain permafrost still exists in the alpine tundra.

5.4. Implications of model uncertainty

Front Range periglacial landforms, which experience freeze–thaw processes, have the potential to modify the geochemistry of alpine lakes and streams. In the Loch Vale watershed, talus is the primary groundwater reservoir; ice stored within permafrost and rock glaciers is the second largest groundwater reservoir (Clow et al., 2003). Storage capacity of talus is equal to or greater than the total annual discharge from the basin (Clow et al., 2003). Talus fields contribute to more than 40% of total discharge during the summer in the Green Lakes 4 catchment (Liu et al., 2004). Rock glacier outflow from the Green Lakes 5 rock glacier in September indicates substantial contributions of magnesium, calcium, and sulfate compared to other surface water sites (Williams et al., 2006). September base flow from the rock glacier also has high nitrate concentrations (Williams et al., 2007). In the Green Lakes Valley, nitrate accounts for 40–90% of total nitrogen (Hood et al., 2003). In Rocky Mountain National Park, a threshold has

Table 5
Areal estimates of permafrost according to each model.

	Area (km^2)	Percentage of study area (%)
Original model	5.08	19.2
Temperature at top of permafrost model	4.62	17.4
Frost number model	1.99	7.5
Common to the original and temperature at the top of permafrost model	2.08	7.8
Common to the frost number and temperature at the top of permafrost model	1.68	6.4
Common to the original and frost number model	0.86	3.2
Common to all models	0.75	2.8

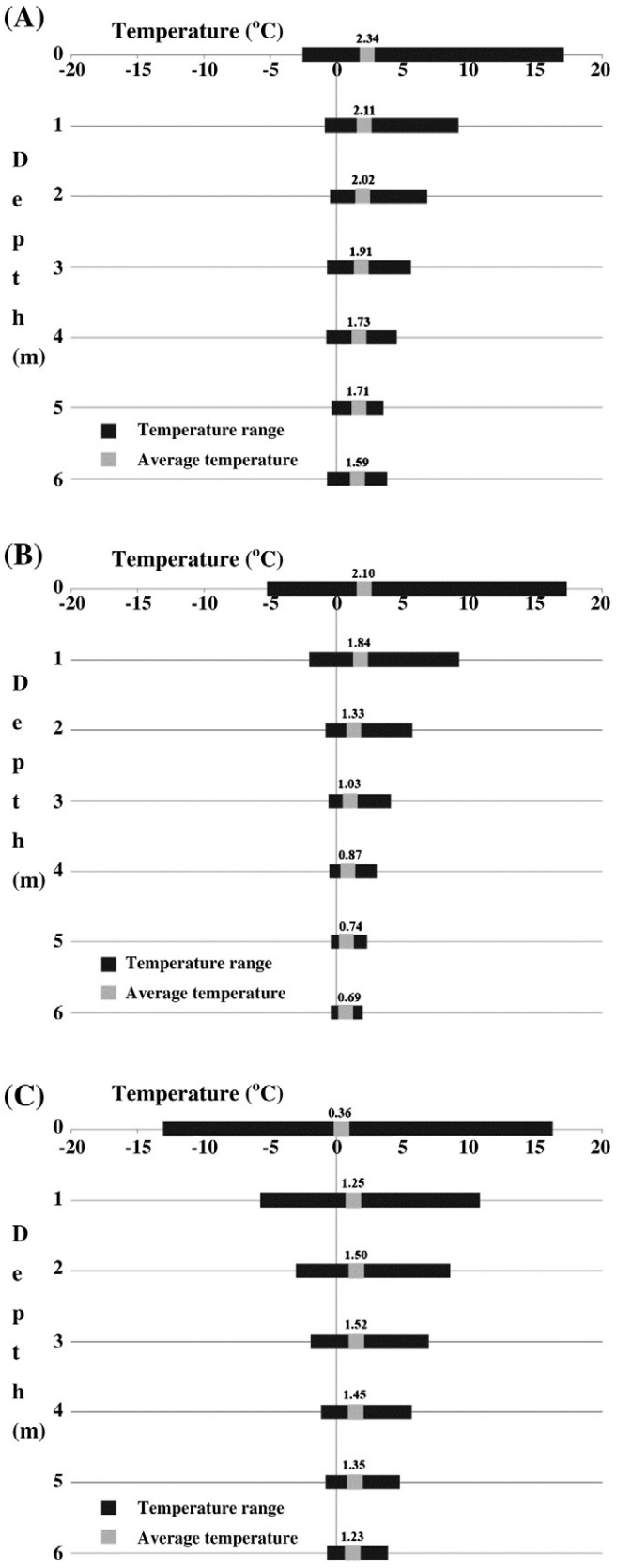

Fig. 6. Temperature measurements for (A) borehole 1, (B) borehole 2, and (C) borehole 3. Mean annual temperature from July 2010 to July 2011 is provided in bold.

apparently been crossed. In the Loch Vale watershed, mean wet nitrogen deposition has not increased; but mean annual net export has increased, suggesting that melting ice in glaciers and rock glaciers has exposed sediments from which nitrogen can be flushed (Baron et al., 2009). The role of thawing ice from permafrost in the Loch Vale catchment is not known, but results suggest that melting of ice within permafrost may contribute to the export of nitrate. The uncertainty among permafrost models makes it difficult to estimate potential future nutrient contributions from warming soils.

According to data from SNOTEL sites across Colorado, annual median air temperatures have increased 0.7 °C per decade from 1986 to 2007 (Clow, 2010). In the Loch Vale watershed, temperatures have increased 1.3 °C per decade from 1983 to 2007 (Clow, 2010). Over the same period, the D-1 station on Niwot Ridge has warmed by 1.0 °C per decade (Clow, 2010). The time period analyzed, however, is an important consideration. Short-term cooling anomalies superimposed on a longer warming trend may cause misinterpretation (Pepin and Losleben, 2002). If air temperatures continue to rise, greater rates of subsidence should be expected. However, this depends upon how much ice underlies a feature. Thus far, no large subsurface segregated-ice structures have been found along TRR, despite historical construction reports that show evidence of ice. If permafrost exists, the majority is likely to be dry and contain forms of pore ice. Therefore, it is more likely that freeze–thaw processes will affect TRR more so compared to melting ice within permafrost.

A changing climate will affect the timing and rate of important ecological processes, including those that correspond to changes in active-layer thickness; therefore, accurately modeling and representing the distribution of permafrost is important. Permafrost soils contain nearly twice as much carbon as the atmosphere. When these soils thaw, large quantities of carbon are lost through decomposition, mainly in the form of methane and carbon dioxide (Lee et al., 2010; Maslin et al., 2010). According to Waldrop et al. (2010), respiration is higher in permafrost soils compared to active layer soils; this suggests that a positive feedback to warming exists. Findings in Siberia, Alaska, and northern Sweden imply that soil carbon that was once stored in deep permafrost is now being released but is likely not the case in the Colorado Rockies (Kuhry et al., 2010). Recently, permafrost soils have also been shown to release nitrous oxides (Elberling et al., 2010). Helmig et al. (2009) found that concentrations of nitrogen oxide were highest at the bottom of the snowpack, which suggests that subnival soils are the origin.

The timing, depth, and duration of snowpack have been shown to influence both existences of permafrost as well as ecological processes. The annual carbon budget can be influenced by the respiratory loss of carbon dioxide from snow microbes beneath the snowpack. According to climatic data from Europe and the western USA, increases in moisture availability and soil temperature have resulted in a sixfold increase in carbon dioxide respiration, despite only a 0.3 to 0.5 °C increase in temperature (Monson et al., 2006). Soil respiration will also be affected by changing snow cover. Over one-half of the carbon assimilated by the montane forest during the summer could be lost by the following winter. Reduced snowpack leads to colder ground temperatures during winter, which decreases the rate of soil respiration. Alpine tundra shows lower total carbon dioxide uptake over shorter periods compared to forested sites; however, alpine tundra has greater total respiration over longer periods (Blanken et al., 2009). The depth of the snowpack may be a more important factor affecting release of carbon compared to warming temperatures (Monson et al., 2006).

6. Conclusions

Soils along TRR remain frozen for the majority of the year. In fact, only two of thirty sites had an average temperature >0 °C at the surface. Sites with colder temperatures tended to have steeper slopes and convex curvatures, suggesting that limited accumulation of snow and coarse debris create an environment that is more conductive of permafrost formation. Frost numbers averaged 0.56 for all sites that are frozen for the majority of days in a year. The TTOP model suggested permafrost at all but one location, with a mean value of −1.8 °C for all sites. However, three boreholes drilled next to TRR indicate no permafrost presence. If permafrost does exist, it is likely to be sporadic and dry (ice-free) at isolated locations.

Mapping and monitoring of permafrost in alpine ecosystems will continue to be a topic of interest as human development increases in the Rocky Mountains. In North America, some researchers have used the −1 °C MAAT isotherm to approximate the lower limit of discontinuous permafrost, whereas other researchers have used the 0 °C MAAT isotherm (Ives, 1974; Washburn, 1980; Nelson and Outcalt, 1987). The analysis presented here suggests a similar conundrum with alpine permafrost. Explicit guidelines are needed to make comparisons between mountainous regions to assess potential impacts in a changing environment.

Questions as to the proper scale, model inputs, and resulting uncertainty remain. Multicriteria GIS techniques that have utilized ground temperatures, land-cover data, and validation by DC resistivity data have been shown to be a good approach for mapping at both the regional and local scale (Etzelmüller et al., 2006). Each of the models presented here has a variety of tradeoffs. Proxy indicator models should be used as a first cut to determine probable locations because of their simplicity and affordability. Regional, macroscale proxy data may generalize; but local, site-specific derived models, such as the frost number and TTOP, may be difficult to regionalize. Spatial interpolation may not be possible and may be misleading given high variability of the alpine temperatures and landcover classes. Geophysical methods such as ground penetrating radar (GPR) or electrical conductivity (EC) methods could help provide a better approximation of the spatial variability of permafrost along TRR. These nonobstructive, two-dimensional and three dimensional methods cover a larger region along transects compared to isolated sample points used in this study, but high purchasing or renting costs place a burden on managers in which they may not be willing to invest (Vonder Mühll et al., 2002; Hauck and Vonder Mühll, 2003). Geophysical methods could also be used temporally to monitor freeze–thaw processes over yearly periods or over the course of seasons (Riseborough et al., 2008; Schrott and Sass, 2008). Thicker active layers and warming soils could provide early signs of climate change in the alpine ecosystem. Uncertainty makes assessing greenhouse gas and nutrient contributions from the alpine environment difficult. A better regional representation of frost-affected soils is needed so that the magnitude of potential ecological change can be better assessed.

Supplementary materials related to this article can be found online at doi: 10.1016/j.geomorph.2011.08.029.

Acknowledgments

Special thanks are given to the National Park Service, in particular Judy Visty and Cheri Yost, for providing financial and administrative support as well as a research permit to conduct this project (Rocky Mountains Cooperative Ecosystem Studies Unit (RM-CESU) Cooperative Agreement Number H12000040001 and RM-CESU Cooperative Agreement Number: H1200090004). Field and laboratory assistants from Metropolitan State College of Denver helped gather, interpret, and analyze the data for this project. Rebecca Brice, Clinton Whitten, Luke Stucker, Loren Sorber, Jessica Taylor, Paschal Jennings, Tricia Dienstfrei, Craig Dreiling, and the members of my GEL 3420 soils class were vital to this project. Additional thanks are extended to the Park Service employees, Ansel and Robert, for their help in the field and transportation to the field sites. Sam Outcalt, Jack Vitek, and an anonymous reviewer greatly improved this manuscript by providing their expert feedback.

Please cite this article as: Janke, J.R., et al., A comparison of permafrost prediction models along a section of Trail Ridge Road, Rocky Mountain National Park, Colorado, USA, Geomorphology (2011), doi:10.1016/j.geomorph.2011.08.029

References

Abu-Hamdeh, N.H., Reeder, R.C., 2000. Soil thermal conductivity: effects of density, moisture, salt concentration, and organic matter. Soil Sci. Soc. Am. J. 64, 1285–1290.

Baron, J.S., Denning, A.S., 1993. The influence of mountain meteorology on precipitation chemistry at low and high elevations of the Colorado Front Range. Atmos. Environ. 27A, 2337–2349.

Baron, J.S., Schmidt, T.M., Hartman, M.D., 2009. Climate-induced changes in high elevation stream nitrate dynamics. Glob. Change Biol. 15, 1777–1789.

Blanken, P.D., Williams, M.W., Burns, S.P., Monson, R.K., Knowles, J., Chowanski, K., Ackerman, T., 2009. A comparison of water and carbon dioxide exchange at a windy alpine tundra and subalpine forest site near Niwot Ridge, Colorado. Biogeochemistry 95, 61–76.

Bonnaventure, P.P., Lewkowicz, A.G., 2008. Mountain permafrost probability mapping using the BTS method in two climatically dissimilar locations, northwest Canada. Can. J. Earth Sci. 45, 443–455.

Brenning, A., Gruber, S., Hoelzle, M., 2005. Sampling and statistical analyses of BTS measurements. Permafrost Periglac. Process. 16, 383–393.

Caine, N., 2011. Recent hydrologic change in a Colorado alpine basin: an indicator of permafrost thaw? Ann. Glaciol. 51, 130–134.

Clow, D.W., 2010. Changes in the timing of snowmelt and streamflow in Colorado: a response to recent warming. J. Clim. 23, 2293–2306.

Clow, D.W., Schrott, L., Webb, R., Campbell, D.H., Torizzo, A., Dornblaser, M., 2003. Ground water occurrence and contributions to streamflow in an alpine catchment, Colorado Front Range. Ground Water — Watershed Issue 41, 937–950.

Damm, B., Langer, M., 2006. Mapping and regionalisation of permafrost phenomena as a basis for natural hazard analyses in south Tyrol (Italy). Mitt. Der Osterreichischen Geog. Ges. 148, 295–314.

Degenhardt, J.J., 2009. Development of tongue-shaped and multilobate rock glaciers in alpine environments — interpretations from ground penetrating radar surveys. Geomorphology 109, 94–107.

Elberling, B., Christiansen, H.H., Hansen, B.U., 2010. High nitrous oxide production from thawing permafrost. Nat. Geosci. 3, 332–335.

Erickson, T.A., Williams, M.W., Winstral, A., 2005. Persistence of topographic controls on the spatial distribution of snow in rugged mountain terrain, Colorado, United States. Water Resour. Res. 41, W04014.

Etzelmüller, B., Heggem, E.S.F., Sharkhuu, N., Frauenfelder, R., Kaab, A., Goulden, C., 2006. Mountain permafrost distribution modelling using a multi-criteria approach in the Hovsgol area, northern Mongolia. Permafrost Periglac. Process. 17, 91–104.

Etzelmüller, B., Farbrot, H., Gudmundsson, A., Humlum, O., Tveito, O.E., Bjornsson, H., 2007. The regional distribution of mountain permafrost in Iceland. Permafrost Periglac. Process. 18, 185–199.

Fukui, K., Sone, T., Strelin, J.A., Toriell, C.A., Mori, J., Fujii, Y., 2008. Dynamics and GPR stratigraphy of a polar rock glacier on James Ross Island, Antarctic Peninsula. J. Glaciol. 54, 445–451.

Grosse, G., Schirrmeister, L., Kumitsky, V.V., Hubberten, H.W., 2005. The use of corona images in remote sensing of periglacial geomorphology: an illustration from the NE Siberian coast. Permafrost Periglac. Process. 16, 163–172.

Gruber, S., Hoelzle, M., 2001. Statistical modelling of mountain permafrost distribution: local calibration and incorporation of remotely sensed data. Permafrost Periglac. Process. 12, 69–77.

Hachem, S., Allard, M., Duguay, C., 2009. Using the MODIS land surface temperature product for mapping permafrost: an application to northern Quebec and Labrador, Canada. Permafrost Periglac. Process. 20, 407–416.

Haeberli, W., 1985. Creep of mountain permafrost: internal structure and flow of alpine rock glaciers. Mitt. Der Versuch. Fur Wasserbau Hydrol. Und Glaziol. 77, 142.

Hauck, C., Vonder Mühll, D., 2003. Inversion and interpretation of two-dimensional geoelectrical measurements for detecting permafrost in mountainous regions. Permafrost Periglac. Process. 14, 305–318.

Helmig, D., Seok, B., Williams, M.W., Hueber, J., Sanford, R., 2009. Fluxes and chemistry of nitrogen oxides in the Niwot Ridge, Colorado, snowpack. Biogeochemistry 95, 115–130.

Hoelzle, M., Haeberli, W., Keller, F., 1993. Application of BTS-measurements for modelling mountain permafrost distribution. Proc. of the VIth Int. Conf. on Permafrost, Beijing, China, pp. 272–277.

Hoffman, M.J., Fountain, A.G., Achuff, J.M., 2007. 20th-century variations in area of cirque glaciers and glacierets, Rocky Mountain National Park, Rocky Mountains, Colorado, USA. Ann. Glaciol. 46, 349–354.

Hood, E., McKnight, D.M., Williams, M.W., 2003. Sources and chemical character of dissolved organic carbon across an alpine/subalpine ecotone, Green Lakes Valley, Colorado Front Range, United States. Water Resour. Res. 39, 1188.

Isaksen, K., Sollid, J.L., Holmlund, P., Harris, C., 2007. Recent warming of mountain permafrost in Svalbard and Scandinavia. J. Geophys. Res.-Earth Surf. 112, F02S04.

Ives, J.D., 1974. Permafrost. In: Ives, J.D., Barry, R. (Eds.), Arct. and Alp. Env. Harper and Row Publishers, New York, pp. 159–194.

Ives, J.D., Fahey, B.D., 1971. Permafrost occurrence in the Front Range, Colorado Rocky Mountains, U.S.A. J. Glaciol. 10, 105–111.

Janke, J.R., 2005a. The occurrence of alpine permafrost in the Front Range of Colorado. Geomorphol. 67, 375–389.

Janke, J.R., 2005b. Modeling past and future alpine permafrost distribution in the Colorado Front Range. Earth Surf. Process. Landf. 30, 1495–1508.

Kuhry, P., Dorrepaal, E., Hugelius, G., Schuur, E.A.G., Tarnocai, C., 2010. Potential remobilization of belowground permafrost carbon under future global warming. Permafrost Periglac. Process. 21, 208–214.

Lantz, T.C., Kokelj, S.V., 2008. Increasing rates of retrogressive thaw slump activity in the Mackenzie Delta region, NWT, Canada. Geophys. Res. Lett. 35, L06502.

Lee, H., Schuur, E.A.G., Vogel, J.G., 2010. Soil CO_2 production in upland tundra where permafrost is thawing. J. Geophys. Res.-Biogeosci. 115, G01009.

Leopold, M., Dethier, D., Volkel, J., Raab, T., 2008. Combining sediment analysis and seismic refraction to describe the structure, thickness and distribution of periglacial slope deposits at Niwot Ridge, Rocky Mountains Front Range, Colorado, USA. Z. Für Geomorphol. 52, 77–94.

Leopold, M., Voelkel, J., Dethier, D., Williams, M.W., Caine, N., 2010. Mountain permafrost — a valid archive to study climate change? Examples from the Rocky Mountains Front Range of Colorado, USA. Nova Acta Leopoldina NF 112, 281–289.

Lewkowicz, A.G., Bonnaventure, P.R., 2008. Interchangeability of mountain permafrost probability models, northwest Canada. Permafrost Periglac. Process. 19, 49–62.

Lewkowicz, A.G., Ednie, M., 2004. Probability mapping of mountain permafrost using the BTS method, Wolf Creek, Yukon Territory, Canada. Permafrost Periglac. Process. 15, 67–80.

Liu, F.J., Williams, M.W., Caine, N., 2004. Source waters and flow paths in an alpine catchment, Colorado Front Range, United States. Water Resour. Res. 40, W09401.

Maslin, M., Owen, M., Betts, R., Day, S., Dunkley Jones, T., Ridgwell, A., 2010. Gas hydrates: past and future geohazard? Philos. Trans. R. Soc. A-Math. Phys. Eng. Sci. 368, 2369–2393.

Monson, R.K., Lipson, D.L., Burns, S.P., Turnipseed, A.A., Delany, A.C., Williams, M.W., Schmidt, S.K., 2006. Winter forest soil respiration controlled by climate and microbial community composition. Nature 439, 711–714.

Munroe, J.S., Doolittle, J.A., Kanevskiy, M.Z., Hinkel, K.M., Nelson, F.E., Jones, B.M., Shur, Y., Kimble, J.M., 2007. Application of ground-penetrating radar imagery for three-dimensional visualisation of near-surface structures in ice-rich permafrost, Barrow, Alaska. Permafrost Periglac. Process. 18, 309–321.

Nelson, F.E., Outcalt, S.I., 1987. A computational method for prediction and prediction and regionalization of permafrost. Arct. Alp. Res. 19, 279–288.

Nyenhuis, M., Hoelzle, M., Dikau, R., 2005. Rock glacier mapping and permafrost distribution modelling in the Turtmanntal, Valais, Switzerland. Z. Für Geomorphol. 49, 275–292.

Pepin, N., Losleben, M., 2002. Climate change in the Colorado Rocky Mountains: free air versus surface temperature trends. Int. J. Climatol. 22, 311–329.

Pieracci, K., Lambiel, C., Reynard, E., 2008. Permafrost distribution in three alpine talus slopes of the Dent de Morcles Massif (Valais, Swiss Alps). Geomorphol.-Relief Process. Environ. 87–97.

Ridefelt, H., Etzelmuller, B., Boelhouwers, J., Jonasson, C., 2008. Statistic-empirical modelling of mountain permafrost distribution in the Abisko region, sub-arctic northern Sweden. Nor. J. Geogr. 62, 278–289.

Riseborough, D., Shiklomanov, N., Etzelmuller, B., Gruber, S., Marchenko, S., 2008. Recent advances in permafrost modelling. Permafrost Periglac. Process. 19, 137–156.

Schrott, L., Sass, O., 2008. Application of field geophysics in geomorphology: advances and limitations exemplified by case studies. Geomorphology 93, 55–73.

Smith, M.W., Riseborough, D., 2002. Climate and the limits of permafrost: a zonal analysis. Permafrost Periglac. Process. 13, 1–15.

Smits, K.M., Sakaki, T., Limsuwat, A., Illangasekare, T.H., 2010. Thermal conductivity of sands under varying moisture and porosity in drainage-wetting cycles. Vadose Zone J. 9, 172–180.

Vonder Mühll, D., Hauck, C., Gubler, H., 2002. Mapping of mountain permafrost using geophysical methods. Prog. Phys. Geogr. 26, 643–660.

Waldrop, M.P., Wickland, K.P., White, R., Berhe, A.A., Harden, J.W., Romanovsky, V.E., 2010. Molecular investigations into a globally important carbon pool: permafrost-protected carbon in Alaskan soils. Glob. Change Biol. 16, 2543–2554.

Washburn, A.L., 1980. Geocryology: A Survey of Periglacial Processes and Environments. Halsted Press, New York, p. 406.

Williams, M.W., 2009. Climate Change Impacts on the Hydrology of High-elevation Catchments. Eur. Geophys. Union Annu. Meet., Vienna, Austria.

Williams, P.J., Smith, M.W., 1989. The Frozen Earth: Fundamentals of Geocryology. Cambridge University Press, New York, p. 306.

Williams, M.W., Knauf, M., Caine, N., Liu, F., Verplanck, P.L., 2006. Geochemistry and source waters of rock glacier outflow Colorado Front Range. Permafrost Periglac. Process. 17, 13–33.

Williams, M.W., Knauf, M., Cory, R., Caine, N., Liu, F., 2007. Nitrate content and potential microbial signature of rock glacier outflow Colorado Front Range. Earth Surf. Process. Landf. 32, 1032–1047.

Williams, M.W., Helmig, D., Blanken, P., 2009. White on green: under-snow microbial processes and trace gas fluxes through snow, Niwot Ridge, Colorado Front Range. Biogeochemistry 95, 1–12.

Please cite this article as: Janke, J.R., et al., A comparison of permafrost prediction models along a section of Trail Ridge Road, Rocky Mountain National Park, Colorado, USA, Geomorphology (2011), doi:10.1016/j.geomorph.2011.08.029